Am J Transl Res 2018;10(9):2940-2948
www.ajtr.org /ISSN:1943-8141/AJTR0071087

Original Article

Peptide nucleic acids targeting mitochondria enhances sensitivity of lung cancer cells to chemotherapy

Sheng-Song Chen*, Xiao-Yun Tu*, Li-Xia Xie, Lv-Ping Xiong, Juan Song, Xiao-Qun Ye

*Department of Respiratory Diseases, The Second Affiliated Hospital of Nanchang University, Nanchang, China. *Equal contributors.*

Received December 17, 2017; Accepted July 14, 2018; Epub September 15, 2018; Published September 30, 2018

Abstract: Acquired resistance to chemotherapy is a major limitation for the successful treatment of lung cancer. Previously, we and others showed that formation of tumor spheres is associated with chemotherapy resistance in lung cancer cells, but the underlying mechanisms remained largely unknown. In the current study, we show that mitochondrial activity is significantly higher in A549 tumor spheres versus monolayer cells, establishing mitochondria as a putative target for antitumor therapy. To this end, we designed a peptide nucleic acids (PNAs) coupled with triphenylphosphonium (TPP) to target the displacement loop (D-loop) regulatory region of mitochondrial DNA (PNA-mito). Treatment with PNA-mito significantly disrupted mitochondrial gene expression, inhibited membrane potential and mitochondria fusion, resulting in proliferation inhibition and cell death. Consistently, in mouse xenograft models, PNA-mito could efficiently inhibit mitochondrial gene expression and block tumor growth. Treatment with a low dose of PNA-mito could significantly enhance the chemotoxicity of cisplatin (CDDP) in drug-resistant A549 tumor spheres. These results establish mitochondria-targeting PNAs as a novel strategy to enhance the accumulative therapeutic outcome of lung cancer.

Keywords: Peptide nucleic acids, lung cancer, tumor spheres, mitochondria

Introduction

Lung cancer is the leading cause of cancer death and non-small cell lung cancer (NSCLC) accounts for more than 85% of all lung cancer cases [1, 2]. Although chemotherapy plays a significant role in lung cancer treatment, prolonged treatment inevitably produces tumors with drug resistance [3]. Accordingly, understanding the molecular mechanisms underlying tumor drug resistance is critical to development of novel and efficient therapeutic strategies for lung cancer treatment.

Cancer stem cells hypothesis proposes that tumors are composed of a functionally heterogeneous cell population derived from the same origin, namely, cancer stem cells (CSCs). Oncological treatments via radiotherapy and/or chemotherapy, however, are usually not able to fully eliminate the lung CSCs, which have a higher self-renewal ability and are protected by specific resistance mechanisms. Surviving CSCs could give rise to new tumors with acquired resistance to anticancer therapies, causing relapse of the disease and therapeutic failures [4, 5]. Accordingly, development of efficient therapies targeting CSCs might be a promising treatment option targeting drug-resistant cancer cells [6]. To study the function of lung CSCs, we previously established a non-adhesive culture system, in which tumor spheres were generated from human A549 lung cancer cells in serum-free mediums [7]. Our results showed that tumor spheres expressed multiple stem cell markers and exhibited higher self-renewal ability and increased drug resistance compared to A549 monolayer cells [7], making it a robust model to study chemotherapy resistance *in vitro*.

Mitochondria are organelles that orchestrate a large number of fundamental cellular functions such as ATP generation and programmed cell death. Deregulation of mitochondrial biogenesis and functionalities have been implicated in tumorigenesis and chemotherapy resistance in multiple tumors. Mitochondrial dynamics is

tightly regulated by fusion and fission protein, which directly affect cell proliferation, energy metabolism, apoptosis, cell invasion and migration [8, 9]. Recently, growing evidence suggests that mitochondrial division and fusion play a critical role in tumorigenesis and regulating sensitivity to chemotherapy [10, 11]. Mitochondrial fusion forms a long reticular structure, which favors energy metabolism [12] and allows mitochondrial genome exchange to maintain mitochondrial DNA stability [13]. Mitochondrial fusion and division are regulated in a cell cycle-dependent manner and are affected by various physiological or pathological stimuli [14, 15]. Notably, it has been shown that mitochondrial fusion protects tumor cells from apoptosis and CSCs exhibit high levels of mitochondrial fusion [14-16]. Consistently, increasing evidence supports the implications of mitochondrial process in regulating drug-resistance in multiple human cancers [17-20].

Peptide nucleic acid (PNA) is a synthetic, nucleic acid analogue in which the sugar backbone is replaced by a neutral peptide-like N-(2-aminoethyl) glycine skeleton. It can bind to both DNA and RNA targets in a sequence-specific manner with high efficiency to form a Watson-Crick type double helix [21], resulting in disruption of transcription or RNA degradation. Mitochondrial DNA (mtDNA) encodes several important proteins involving in mitochondrial fusion and oxidative phosphorylation. mtDNA is double-stranded DNA molecule, which consists of the heavy strand (H) and the light strand (L). Notably, both light-strand promoter (LSP) and heavy-strand promoter (HSP) are localized in displacement loop (D-loop) regulatory region, making it a putative target for PNA interference. We thus designed a PNA for D-loop targeting and coupled the PNA to triphenylphosphonium (TPP), a delocalized lipophilic cation for mitochondria targeting [22, 23]. We then examined the anti-tumor effects of PNA using both *in vitro* and *in vivo* models, and evaluated the effect of combined treatment with cisplatin (CDDP) in drug-resistant A549 tumor spheres.

Materials and methods

Reagents

The PNA was constructed and synthesized by the Korea PANAGENE. PNA sequence targeting the mtDNA (PNA-mito) was designed as 5'-CAGACCGCCAAAAGA-3'; a control PNA with shuffled sequence was designed as 5'-ACGTGTTCCATAACA-3'. PNA were covalently linked to a Triphenylphosphorous (TPP) at the C-terminus. PNA oligos were purified by reverse phase HPLC. Cisplatin was obtained from Sigma-Aldrich and dissolved to 10 M in 0.15 M NaCl. Anti-MFN1 antibody, anti-ATAD3A antibody, anti-ATP6 antibody were purchased from Abcam, β-actin were purchashed from Santa Cruz. Mito-Tracker Green was obtained from Sigma-Aldrich. ATP detection kit, BCA protein assay kit were obtained from Jiangsu Beyotime Rhodamine 123 kit and AnnexinV-FITC detection kit were purchased from Thermo Fisher.

Cell culture and tumor sphere formation

A549 cell line was obtained from American type culture collection (ATCC). A549 cells were cultured in DMEM with 10% fetal bovine serum (FBS). To obtain stem-like sphere cells, the adherent cells were separated from A549 cells and seeded in new 6-well plates at 1×10^3 cells/well with DMEM contained with 10% FBS (Gibco) for more than 2 weeks, the holoclones were selected by using cloning cylinders and plated with serum-free medium (Gibco) containing 4 u/l insulin, 20 μg/l EGF, 20 μg/l bFGF and 1% penicillin/streptomycin. All the cells were maintained in a 37°C humidified incubator containing 5% CO_2.

Western blot

Total protein was extracted using RIPA buffer (50 mM Tris HCl, 150 mM NaCl, 1 mM EDTA, 1% (v/v) Triton-X 100, 0.1% (w/v) SDS) supplemented with phenylmethylsulfonyl fluoride (PMSF) and protease inhibitor cocktail (Roche) at 4°C for 30 min. 20 μg total proteins were separated through 10% SDS-PAGE and wet transferred to the PVDF membranes. After blocking in TBST containing 5% non-fat dry milk for 2 h at room temperature, PVDF membranes were incubated with primary antibodies overnight at 4°C overnight. Membranes were washed 3X with TBST, and incubated with the corresponding secondary antibodies at room temperature for 2 h. Target bands were detected and visualized using SuperSignal enhanced chemiluminescence substrate (Pierce). Whole films of the western blot bands are shown in Supplementary Figure 1.

Animals and xenograft models

3-4 weeks old, 15-20 g, female NOD-SCID mice were purchased from Hunan Slack King of Laboratory Animal Co., Ltd. (certificate of No. 43004700009696), and housed in the SPF IVC environment Department of Animal Science in Nanchang University. All the experiments were approved by the Scientific Ethical Committee of Nanchang University. Xenograft models were established by injecting 5×10^6/0.2 ml A549 cells into the hind groin of nude mice. Tumor volumes were measured in two dimensions using a vernier caliper (the formula length × width^2)/2. Every two days, mice were treated with intratumoral injections of 2 mg/kg PNA oligomers.

Confocal imaging

A549 cells were exposed to 10 μM PNA oligomers for 24 h, then incubated with Mito-Tracker Green solution at 37°C for 10 min. After that, cells were washed 3X with PBS, and fixed with 4% formaldehyde solution in PBS for 15 min. Images were captured using a Yokogawa spinning disk confocal on an inverted Nikon Ti fluorescence microscope.

Flow cytometry

Cells were seeded in 12-well plates for 24 hours and then exposed to different treatment. After that, cells were trypsinized washed twice with PBS, and incubated with AnnexinV-FITC/propidiumiodide or Rhodamine 123 according to manufacturer's instructions. Cell populations were analyzed by a FACSCalibur Flow Cytometer (BD).

Immunohistochemistry

Tumor tissue were fixed in 4% paraformaldehyde and drawn in 20% sucrose solution at 4°C overnight. 3% H_2O_2 was added to block endogenous tissue peroxidase. Slides were permeabilized with 0.3% Triton X-100 in PBS for 10 min, incubated in primary antibody at 4°C overnight, incubated in biotin-labeled secondary antibody for 2 h at room temperature, colored by DAB solution and hematoxylin staining. Images were captured using a Axio Vert A1 inverted fluorescence microscope. Image Pro Plus 6.0 was used for image data processing.

Statistical analysis

SPSS19.0 statistical software was used for the statistical analysis. All experiments were repeated at least three times and representative results were presented. Where applicable, quantitative data were presented as means ± SD. Paired or unpaired Student's t-test were used to determine differences between different groups. $P<0.05$ was considered statistically significant.

Results

High mitochondria activity in A549 tumor sphere

Previously, we and others showed that tumor spheres (**Figure 1A**) derived from NSCLC cell line A549 show increased proliferation, cell-cycle progression as well as drug-resistant properties as compared to cells in monolayer cultures [7]. To investigate their difference in mitochondria activities, we examined expression of several mitochondrial proteins using western blot, including mitochondrial membrane ATP synthases ATP Synthase 6 (ATP6) and ATPase Family AAA Domain-Containing Protein 3A (ATAD3A), as well as mitochondrial outer membrane GTPase Mitofusin 1 (MFN1), which is essential for mitochondrial fusion. Our results showed that the expression levels of ATP6, ATAD3A and MFN1 were consistently upregulated in A549 sphere versus monolayer A549 cells (**Figure 1B**), indicating higher mitochondrial content and activity. We then used Rhodamine123 and flow cytometry to monitor the membrane potential of mitochondria (**Figure 1C**). Consistent with enhanced mitochondrial protein expression, our results suggested that mitochondrial membrane potential is significantly higher in A549 spheres than the A549 cell (**Figure 1D**, $P = 4.23 \times 10^{-7}$, Student's t-test). Together, these results indicate enhanced mitochondrial activity in sphere cultures. This is consistent with hyper activation of mitochondria being important in regulating drug resistance in various tumors.

PNA-mito blocks mitochondrial gene expression and function in vitro

Peptide nucleic acid (PNA) oligomers are nucleic acid analogues that specifically bind to target DNA to block replication and transcription. To

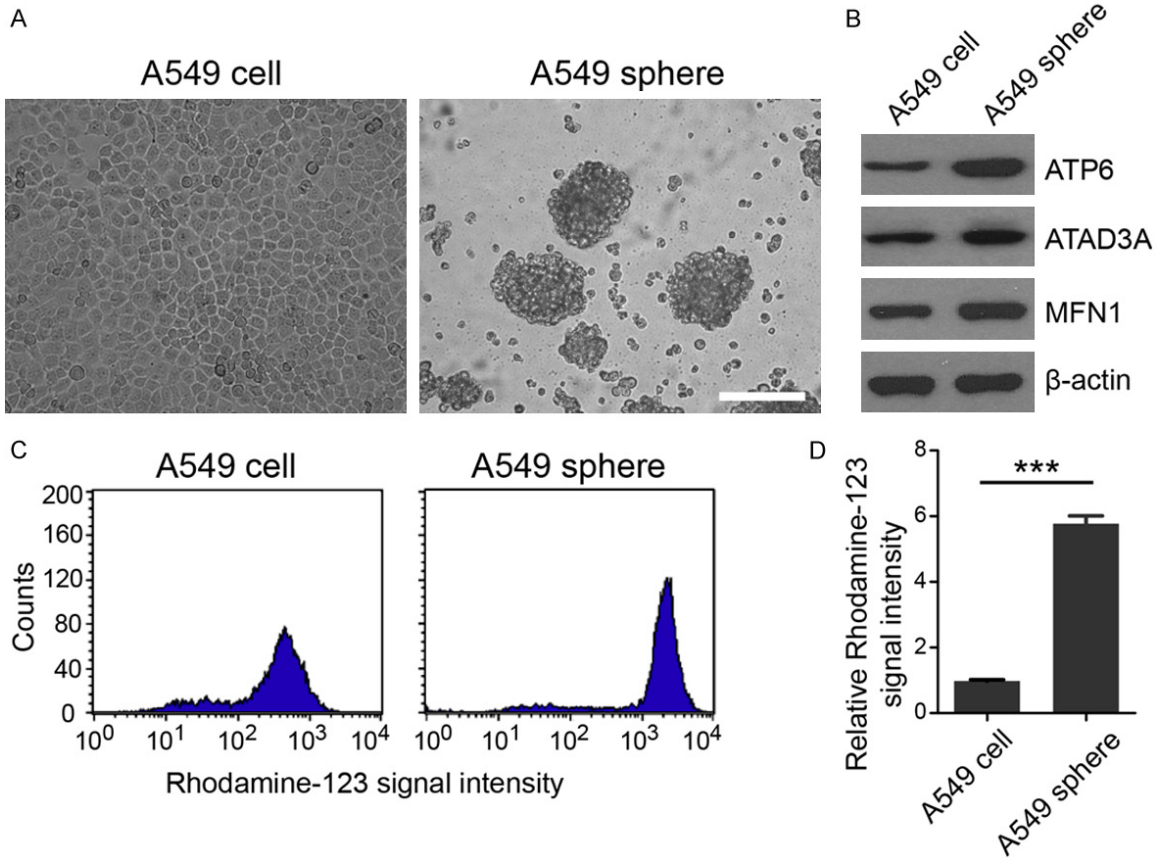

Figure 1. High mitochondria activity in A549 tumor sphere. (A) Morphologies of monolayer A549 cells in regular medium and A549 tumor spheres formed in growth factors-defined serum-free medium. Scale bar: 500 μm. (B) Western blot of ATP6, ATAD3A and MFN1 protein expression in monolayer A549 cells and A549 tumor spheres. (C) Flow cytometry analysis of Rhodamine-123 signal intensities in A549 cells and A549 tumor spheres. (D) Statistics of Rhodamine-123 signal intensities shown in (C). Data show Mean ± SD of three replicates. ***, P<0.001, Student's t-test.

target mitochondria of NSCLC cells, we designed a PNA targeting the displacement loop (D-loop) region of mitochondrial DNA (PNA-mito) and a control oligomer with shuffled sequence (PNA-cntl). Both oligomers were conjugated to TPP to allow efficient trafficking to mitochondria through the lipid bilayer driven by the membrane potential across the inner membrane [23]. Significantly, our results showed that PNA-mito, but not PNA-cntl, could block A549 cell proliferation in a dose-dependent manner (**Figure 2A**). As shown in **Figure 2B**, treatment with 10 μM PNA oligomers for 24 h caused dramatic changes in mitochondria morphology, particularly resulting in blockage of mitochondrial fusion. We then asked whether mt-DNA targeting by PNA could manipulate mitochondrial gene expression and function in cells. As shown in **Figure 2C**, western blot showed that expression of ATP6, ATAD3A and MFN1 were all downregulated in A549 cells treated with PNA-mito compared to those treated with PNA-cntl. Consistently, intracellular ATP concentration were significantly reduced following PNA-mito treatment than control (**Figure 2D**, $P = 3.53 \times 10^{-11}$, Student's t-test). Mitochondria membrane potential, which is an indicator of mitochondrial activity, was likewise repressed following PNA-mito treatment (**Figure 2E**, $P = 2.13 \times 10^{-4}$, Student's t-test). Moreover, our results showed that PNA-mito treatment resulted in significantly enhanced cell death compared to PNA-cntl (**Figure 2F**, $P = 6.06 \times 10^{-13}$, Student's t-test). Together, these results established PNA-mito as a specific inhibitor of mitochondrial gene expression and function, supporting its role as a novel therapeutic approach towards NSCLC treatment.

PNA-mito inhibits tumor growth in vivo

We then examined the effect of PNA-mito on tumor growth *in vivo* using a mouse xenograft

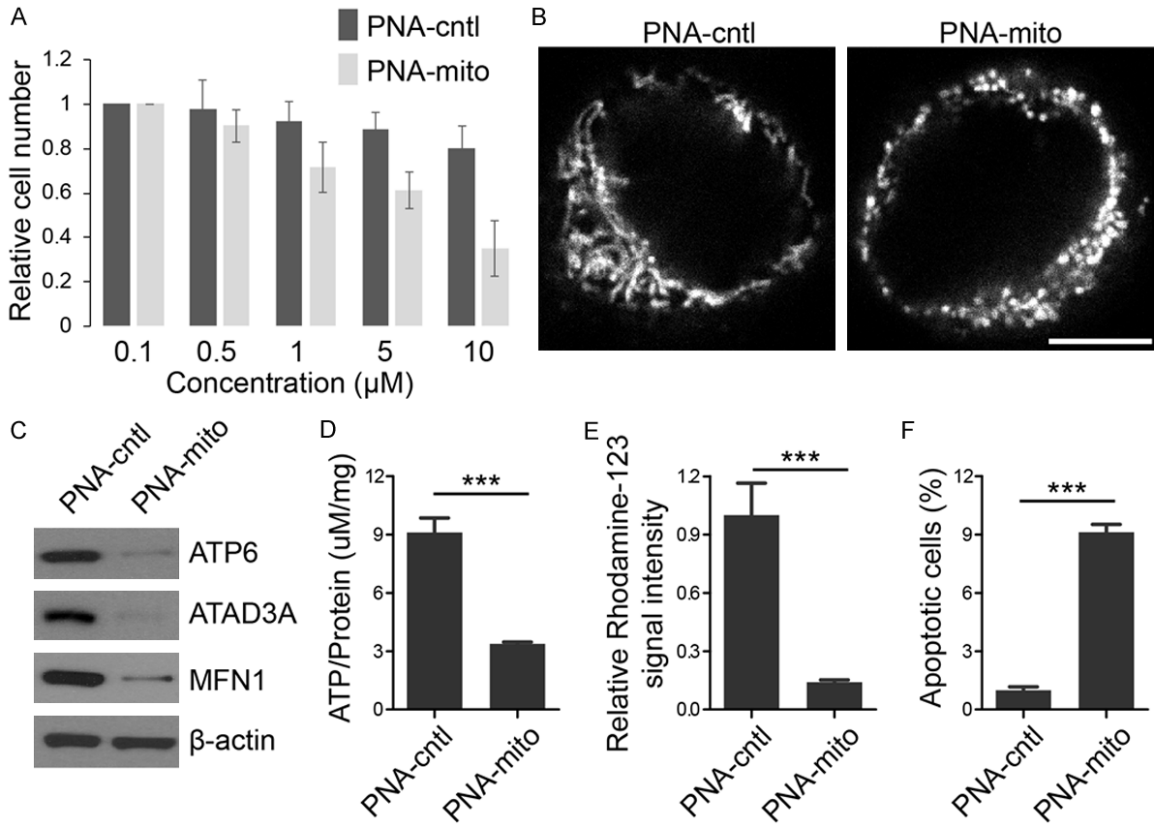

Figure 2. PNA-mito blocks mitochondrial gene expression and function *in vitro*. A. The relative number of cells following treatment with different dose of PNA-mito or PNA-cntl. Data were normalized by cells treated with 0.1 PNA-cntl. B. Staining of mitochondria by MitoTracker in A549 cells treated with 10 μM PNA oligomers for 24 h. Scale bar: 5 μm. C. Western blot of ATP6, ATAD3A and MFN1 protein expression in A549 cells treated with 10 μM PNA oligomers for 24 h. D. ATP concentrations (normalized by total protein abundance) in A549 cells treated with 10 μM PNA oligomers for 24 h. E. Rhodamine-123 signal intensities A549 cells treated with 10 μM PNA oligomers for 24 h. F. The percentage of apoptotic cells following treatment with 10 μM PNA oligomers for 24 h. Data show Mean ± SD of three replicates. ***, P<0.001, Student's t-test.

model, in which mice were subcutaneously implanted with 5×10^6 xenografted A549 cells in the left flank. Seven days following xenograft, mice in the two experimental groups (PNA-mito *vs* PNA-cntl, n = 6 per group) were treated with a daily intra-tumor injection of different PNA oligomers, and toxicity of the PNA oligomers was evaluated by measuring tumor volume every week during a 5-week follow up. Consistent with *in vitro* results, our results showed a potent decrease in tumor volume overtime in mice treated with PNA-mito compared to PNA-cntl (**Figure 3A**, **3B**, $P = 1.67 \times 10^{-10}$, Paired Student's t-test).

To gain a better understanding of the inhibitory activity, we further examined the effects of PNA oligomers on tumor mitochondrial gene expression in the tumor xenografts. Tumors were dissected and target proteins were examined by immunochemistry staining. In line with *in vitro* data, immunohistochemistry showed that PNA-mito treatment significantly reduced expression of ATP6, ATAD3A and MFN1 in tumor xenografts compared to PNA-cntl treatment (**Figure 3C**). This result was further validated by western blot (**Figure 3D**). We thus suggested that PNA-mito oligomers could efficiently target mitochondrial in the tumor xenografts and interfere with mitochondrial gene expression. Together, these results established a promising therapeutic potential for PNA-mito *in vivo*.

A low dose of PNA-mito significantly enhanced the chemotoxicity of cisplatin (CDDP) in drug-resistant A549 tumor spheres

CDDP is one of the most effective anticancer agents for NSCLC treatment via inducing DNA

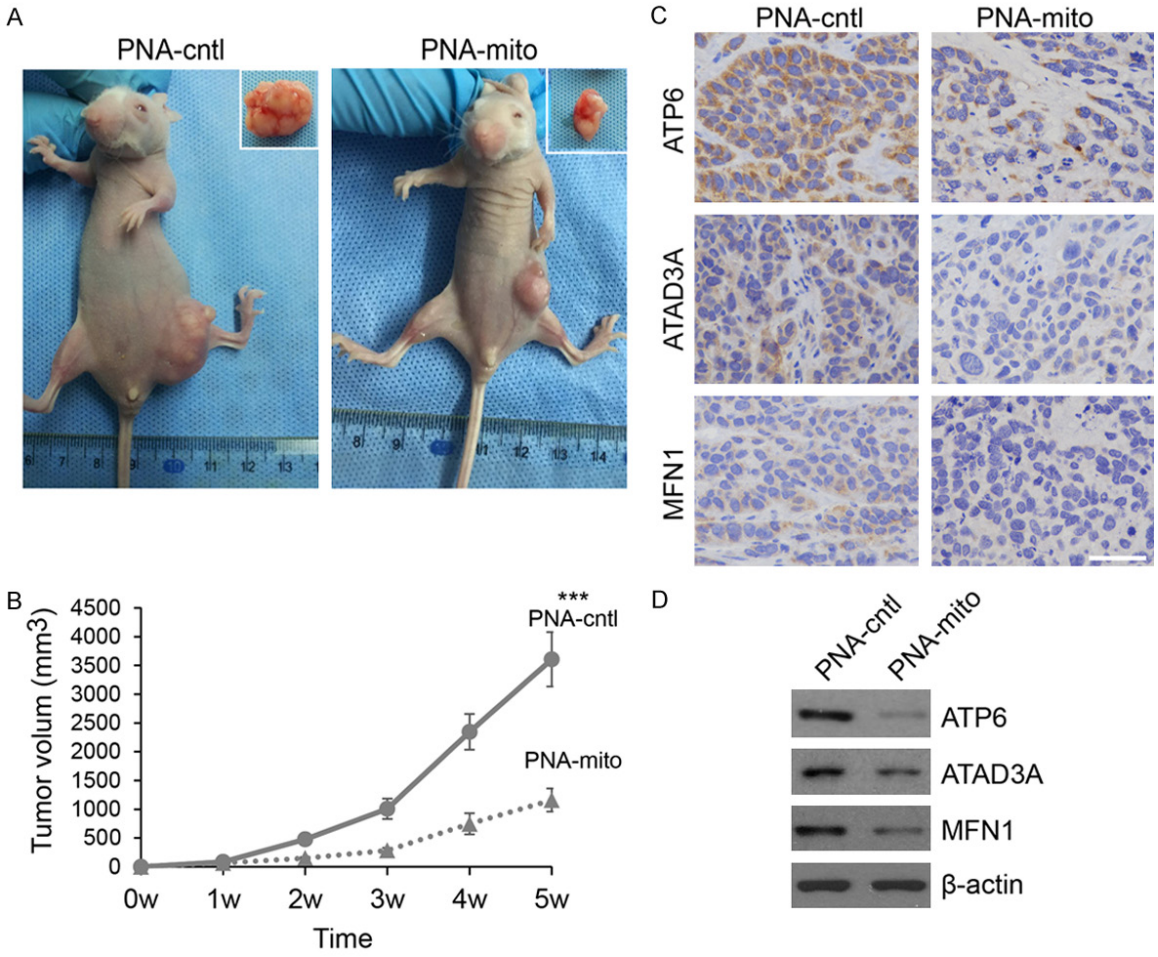

Figure 3. PNA-mito inhibits tumor growth in vivo. (A) Tumors in mice A549 xenograft models following daily intratumor injection of different PNA oligomers for 5 weeks. (B) Tumor growth curve in xenografted mice treated with different PNA oligomers (n=6 per group). Data show Mean±SD. ***, p<0.001, Paired Student's t-test. (C) Immunohistochemistry staining of ATP6, ATAD3A and MFN1 protein expression in A549 xenograft tumors treated with different PNA oligomers. (D) Western blot of ATP6, ATAD3A and MFN1 protein expression in tumors shown in (C).

damage response and inhibition of DNA synthesis. We previously showed that in A549 tumor spheres have higher resistance to CDDP than A549 cells in monolayer culture [7]. It has been hypothesized that mitochondrial content, such as composition of mitochondrial proteins and signal-transducing events, plays a critical role in tumor chemotherapy resistance. In line with this hypothesis, we observed high mitochondrial expression/activity in drug-resistant A549 tumor spheres compared to monolayer A549 cells. We thus asked whether targeting mitochondria of A549 sphere cells using a non-toxic low dose of PNA oligomers might enhance the chemotoxicity of CDDP in these cells. We first treated A549 tumor spheres with increasing concentrations (ranging from 0.01 μM to 80 μM) of CDDP or PNA-mito for 24 h to determine the IC_{50} values (**Figure 4A**, **4B**). Our results revealed that the IC_{50} of CDDP was 43.2 μM and IC_{50} values of PNA-mito was 15.6 μM in these cells (**Figure 4A**). Treatment of A549 cells with a non-toxic low dose of PNA (5 μM) didn't resulted in significant cell death. Notably, however, combined treatment with 5 μM PNA-mito, but not PNA-cntl, could dramatically enhance CDDP-induced cell death in sphere cells as evidenced by reduction in CDDP IC_{50} values (10.3 μM vs 40.2 μM, **Figure 4C**). Notably, as shown in **Figure 4D**, an even lower dose of PNA-mito (1 μM) was sufficient to enhanced the chemotoxicity of CDDP (16.7 μM vs 42.7 μM), highlighting a great synergic antitumor effect between PNA-mito and CDDP.

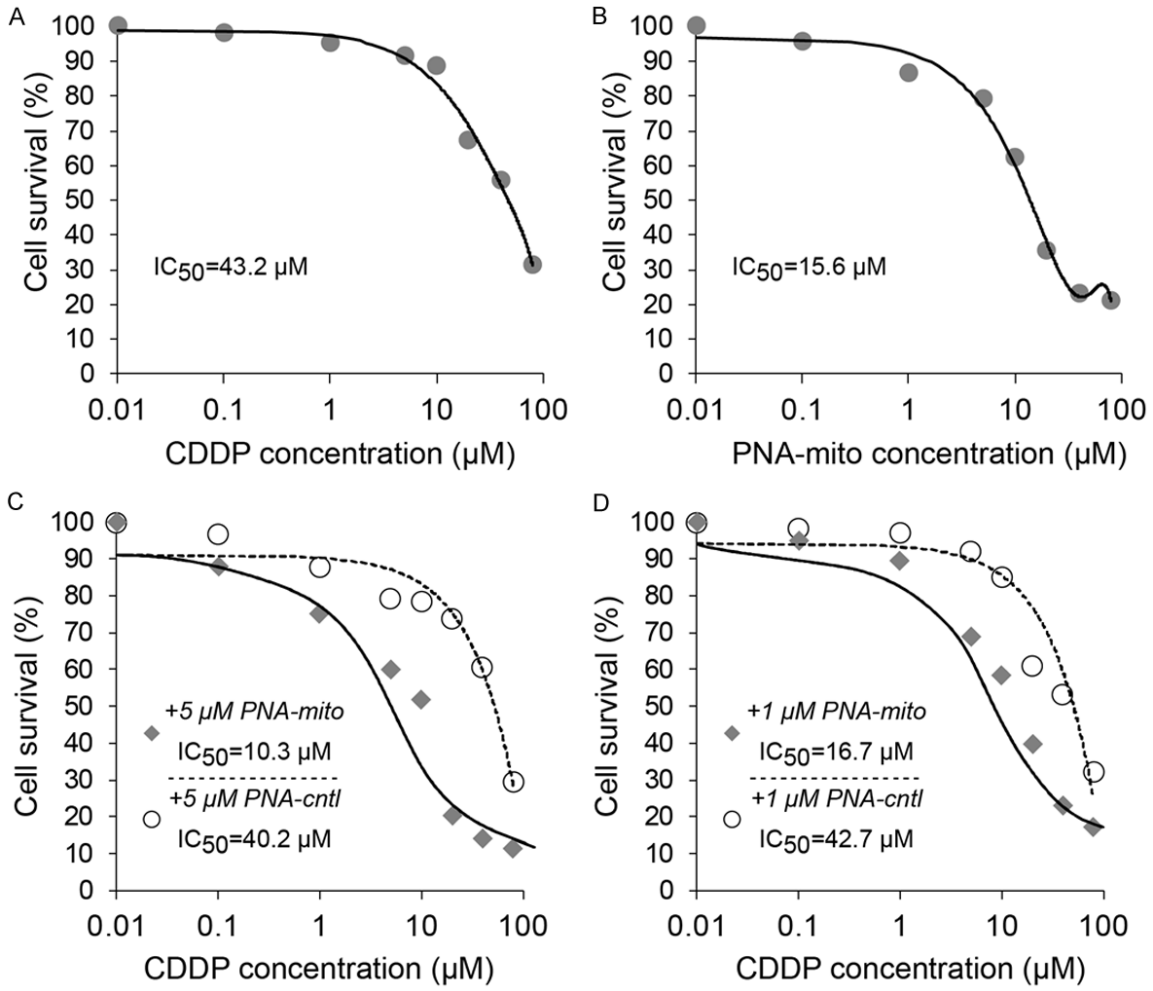

Figure 4. A low dose of PNA-mito significantly enhanced the chemotoxicity of CDDP. A. The dose response curve and the IC_{50} of CDDP in drug-resistant A549 tumor spheres. B. The dose response curve and the IC_{50} of PNA-mito in A549 tumor spheres. C. The dose response curves of CDDP in combination with 5 μM PNA-mito or PNA-cntl in A549 tumor spheres. D. The dose response curve and the IC_{50} of CDDP in combination with 1 μM PNA-mito or PNA-cntl in A549 tumor spheres.

Together, these results suggest the therapeutic potential of mitochondria-targeting PNA as a novel strategy to overcome drug resistance in lung cancer.

Discussion

Platinum-containing drugs combining with chemotherapy was the first-line treatment in advanced lung cancer, however, CDDP-resistance and drug toxicity were the main obstacles of anti-tumor treatment [3, 4]. In the current study, we investigated the function of a mitochondria-targeting PNA oligomers and its implications in combined cancer therapy. Our results showed that PNA-mito could potently disrupted mitochondrial gene expression and function, resulting in proliferation inhibition and cell death of NSCLC A549 cells both *in vitro* and in mouse xenograft models. Moreover, a low dose of PNA-mito could significantly enhance the sensitivity of drug-resistant A549 tumor spheres to CDDP. We thus highlight the therapeutic potential of PNA oligomers as a novel strategy to overcome drug resistance in lung cancer.

There are several putative mechanisms underlying enhanced drug-resistance in tumor cells involving mitochondria. For example, abnormal upregulation of anti-apoptotic proteins such as B-celllymphoma-2 proteins (BCL-2) and/or inhibition of pro-apoptotic proteins (BAX) and BCL-2 homology antagonist (BAK) might enhance cell

survival in response to drug stimuli [24]. Mitochondrial metabolic processes such might reduce reactive oxygen species (ROS) damage induced by chemotherapy or radiation therapy within the cell [16, 17, 20]. Accordingly, PNA-induced disruption of mitochondria gene expression might result in a pro-apoptotic remodeling of mitochondrial content and cell death. Moreover, increasing evidence suggest that mitochondrial fusion is involving in cancer cell resistance to chemotherapy via delaying cytochrome c release upon stimuli [16-20]. In line with this notion, several studies found that embryonic stem cells and pluripotent stem cells exhibit increased mitochondrial fusion [25, 26], suggesting that mitochondrial fusion in A549 sphere cells play an important role in maintaining tumor stemness. In the current study, we found that A549 sphere cells express higher a level of mitochondrial fusion protein MFN1 compared to A549 monolayer cells, supporting the functional relevancy. Notably, treatment with PNA-mito resulted in potent disruption of mitochondrial fusion *in vitro*. In animal models, PNA oligomers demonstrated high stability and great biological compatibility, specifically targeted mitochondria, and efficiently reduced tumor size, providing a valuable tool for overcoming drug-resistance in lung cancer.

In conclusion, our results suggest that PNA oligomers could efficiently inhibit mitochondrial function and enhance CDDP chemotherapy sensitivity in NSCLC. This provides a rationale and a proof-of-concept for developing specific therapeutic targeting and drug combination to enhance the accumulative therapeutic outcome of the disease.

Acknowledgements

This work was supported by the National Natural Science Foundation of China (no 816-60493) and Natural Science Foundation of Jiangxi province (no 20143ACB20011).

Disclosure of conflict of interest

None.

Address correspondence to: Xiao-Qun Ye, Department of Respiratory Diseases, The Second Affiliated Hospital of Nanchang University, Nanchang, China. E-mail: xqyencu@gmail.com

References

[1] Chen W, Zheng R, Baade PD, Zhang S, Zeng H, Bray F, Jemal A, Yu XQ and He J. Cancer statistics in China, 2015. CA Cancer J Clin 2016; 66: 115-132.

[2] Siegel RL, Miller KD and Jemal A. Cancer statistics, 2016. CA Cancer J Clin 2016; 66: 7-30.

[3] Du L and Morgensztern D. Chemotherapy for advanced-stage non-small cell lung cancer. Cancer J 2015; 21: 366-370.

[4] Hainaut P and Plymoth A. Targeting the hallmarks of cancer: towards a rational approach to next-generation cancer therapy. Curr Opin Oncol 2013; 25: 50-51.

[5] Vermeulen L, de Sousa e Melo F, Richel DJ and Medema JP. The developing cancer stem-cell model: clinical challenges and opportunities. Lancet Oncol 2012; 13: e83-89.

[6] Yang Y, Xu H, Huang W, Ding M, Xiao J, Yang D, Li H, Liu XY and Chu L. Targeting lung cancer stem-like cells with TRAIL gene armed oncolytic adenovirus. J Cell Mol Med 2015; 19: 915-923.

[7] Sun FF, Hu YH, Xiong LP, Tu XY, Zhao JH, Chen SS, Song J and Ye XQ. Enhanced expression of stem cell markers and drug resistance in sphere-forming non-small cell lung cancer cells. Int J Clin Exp Pathol 2015; 8: 6287-6300.

[8] Kasahara A and Scorrano L. Mitochondria: from cell death executioners to regulators of cell differentiation. Trends Cell Biol 2014; 24: 761-770.

[9] Schrepfer E and Scorrano L. Mitofusins, from mitochondria to metabolism. Mol Cell 2016; 61: 683-694.

[10] Weinberg SE and Chandel NS. Targeting mitochondria metabolism for cancer therapy. Nat Chem Biol 2015; 11: 9-15.

[11] Ye XQ, Wang GH, Huang GJ, Bian XW, Qian GS and Yu SC. Heterogeneity of mitochondrial membrane potential: a novel tool to isolate and identify cancer stem cells from a tumor mass? Stem Cell Rev 2011; 7: 153-160.

[12] Jourdain A and Martinou JC. Mitochondrial dynamics: quantifying mitochondrial fusion in vitro. BMC Biol 2010; 8: 99.

[13] Chen H, Vermulst M, Wang YE, Chomyn A, Prolla TA, McCaffery JM and Chan DC. Mitochondrial fusion is required for mtDNA stability in skeletal muscle and tolerance of mtDNA mutations. Cell 2010; 141: 280-289.

[14] Trotta AP and Chipuk JE. Mitochondrial dynamics as regulators of cancer biology. Cell Mol Life Sci 2017; 74: 1999-2017.

[15] Senft D and Ronai ZA. Regulators of mitochondrial dynamics in cancer. Curr Opin Cell Biol 2016; 39: 43-52.

[16] Santin G, Piccolini VM, Barni S, Veneroni P, Giansanti V, Dal Bo V, Bernocchi G and Bottone MG. Mitochondrial fusion: a mechanism of cisplatin-induced resistance in neuroblastoma cells? Neurotoxicology 2013; 34: 51-60.
[17] Fan Z, Yu H, Cui N, Kong X, Liu X, Chang Y, Wu Y, Sun L and Wang G. ABT737 enhances cholangiocarcinoma sensitivity to cisplatin through regulation of mitochondrial dynamics. Exp Cell Res 2015; 335: 68-81.
[18] Han XJ, Yang ZJ, Jiang LP, Wei YF, Liao MF, Qian Y, Li Y, Huang X, Wang JB, Xin HB and Wan YY. Mitochondrial dynamics regulates hypoxia-induced migration and antineoplastic activity of cisplatin in breast cancer cells. Int J Oncol 2015; 46: 691-700.
[19] Casinelli G, LaRosa J, Sharma M, Cherok E, Banerjee S, Branca M, Edmunds L, Wang Y, Sims-Lucas S, Churley L, Kelly S, Sun M, Stolz D and Graves JA. N-Myc overexpression increases cisplatin resistance in neuroblastoma via deregulation of mitochondrial dynamics. Cell Death Discov 2016; 2: 16082.
[20] Han XJ, Shi SL, Wei YF, Jiang LP, Guo MY, Wu HL and Wan YY. Involvement of mitochondrial dynamics in the antineoplastic activity of cisplatin in murine leukemia L1210 cells. Oncol Rep 2017; 38: 985-992.
[21] Nielsen PE, Egholm M, Berg RH and Buchardt O. Sequence-selective recognition of DNA by strand displacement with a thymine-substituted polyamide. Science 1991; 254: 1497-1500.
[22] Filipovska A, Eccles MR, Smith RA and Murphy MP. Delivery of antisense peptide nucleic acids (PNAs) to the cytosol by disulphide conjugation to a lipophilic cation. FEBS Lett 2004; 556: 180-186.
[23] Muratovska A, Lightowlers RN, Taylor RW, Turnbull DM, Smith RA, Wilce JA, Martin SW and Murphy MP. Targeting peptide nucleic acid (PNA) oligomers to mitochondria within cells by conjugation to lipophilic cations: implications for mitochondrial DNA replication, expression and disease. Nucleic Acids Res 2001; 29: 1852-1863.
[24] Martinou JC and Youle RJ. Mitochondria in apoptosis: Bcl-2 family members and mitochondrial dynamics. Dev Cell 2011; 21: 92-101.
[25] Chou SJ, Tseng WL, Chen CT, Lai YF, Chien CS, Chang YL, Lee HC, Wei YH and Chiou SH. Impaired ROS scavenging system in human induced pluripotent stem cells generated from patients with MERRF syndrome. Sci Rep 2016; 6: 23661.
[26] Choi HW, Kim JH, Chung MK, Hong YJ, Jang HS, Seo BJ, Jung TH, Kim JS, Chung HM, Byun SJ, Han SG, Seo HG and Do JT. Mitochondrial and metabolic remodeling during reprogramming and differentiation of the reprogrammed cells. Stem Cells Dev 2015; 24: 1366-1373.

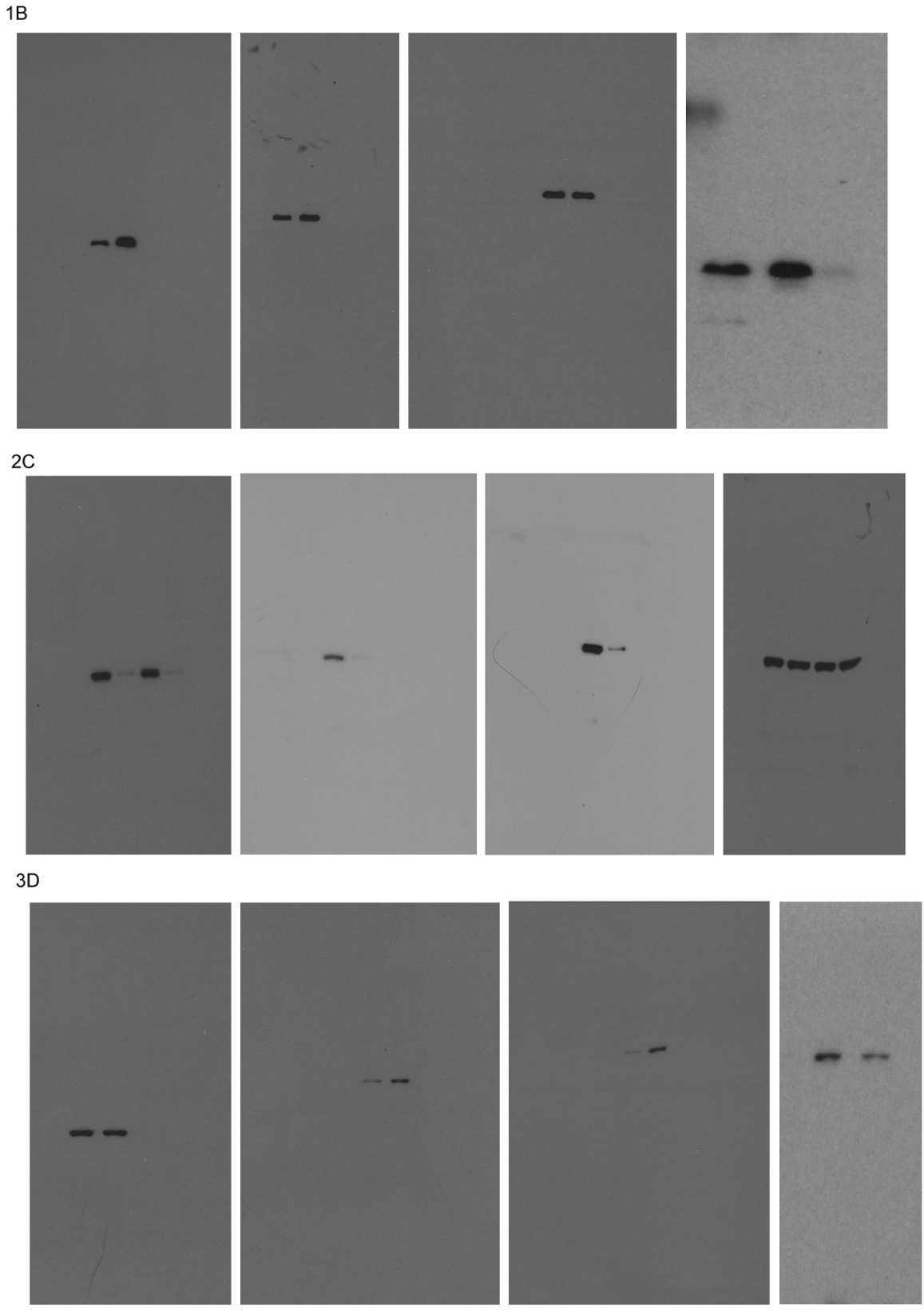

Supplementary Figure 1. Raw data for western blot.